High Temperature Polaritons in Ceramic Nanotube Antennas

Ryan Starko-Bowes,[†] Xueji Wang,[‡] Zhujing Xu,[‡] Sandipan Pramanik,[†] Na Lu,[‡] Tongcang Li,[‡] and Zubin Jacob[*,‡,†]

[†]*University of Alberta, Edmonton, Alberta, Canada*

[‡]*Birck Nanotechnology Center, Purdue University, West Lafayette, Indiana, USA*

E-mail: zjacob@purdue.edu

Supporting Information

Experimental Details

Experimental measurements are performed using a custom high temperature thermal emission vacuum chamber set-up described in reference [1]. IR transmission measurements are performed at room temperature with a Thermo Fisher Scientific Nicolet is50 FTIR spectrometer using the Polaris^{TM}long lifetime IR-source and a mercury cadmium telluride (MCT) detector. Samples are prepared by dispersing multi-walled (MW) BNNTs of average diameter 50 nm and lengths of 5-20 μm on to a polished Si wafer that is partially transmissive from 4-25 μm.

For thermal emission measurements, the BNNT system must be deposited on a refractory low-e thin film to reflect all thermal radiation from the heater and give a low background thermal emission. We deposit a 300 nm tungsten thin on a polished silicon wafer with a 10 nm titanium film for adhesion. First the titaniium layer is deposited at 230 W DC power

with 10 mTorr of argon flowing at 15 sccm. Next, tungsten was deposited at 120 W DC power with 2 mTorr of argon flowing at 15 sccm. The Resulting thin film has a low broadband IR emissivity of 0.1.

During collection of thermally emitted light, we use a gold coated parabolic mirror of focal length 4" (101.6 mm) and a 3mm x 22.86mm slit to define the angular resolution of our measurements. Due to the diffraction limit, our collection area (spot size) will differ depending on the emission peak wavelength. For the two extreme cases we observe a spot size of 285.6 x 37.5 μm for the T mode and 529.7 x 69.5 μm for the RB mode.

Figure S1 shows the experimental set-up used to measure the emissivity spectrum of our system. Detection of thermally generated radiation is permormed using the same Thermo Fisher Scientific Nicolet is50 FTIR spectrometer as before. Again using the MCT detector.

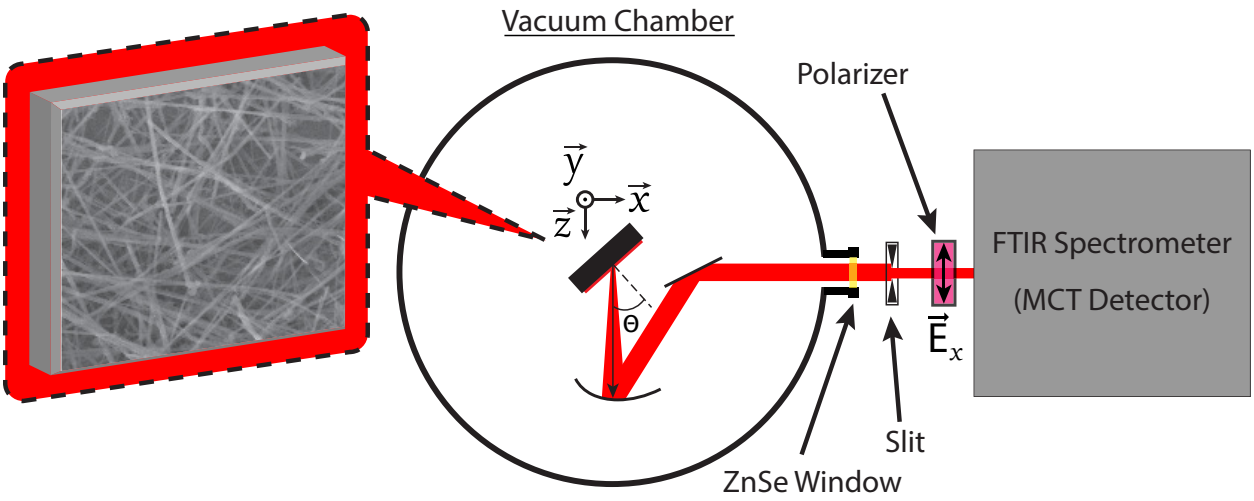

Figure S1: Schematic of experimental set-up used to measure emissivity spectrum.

TEM Characterization

To make the BNNT samples used in this experiment, powder-form BNNTs were purchased from Bonding Chemical. The BNNTs were then dispersed in ethanol and drop-coated onto desired substrates. To characterize the crystalline quality of the nanotubes, TEM images were taken after a standard sample preparation procedure with the BNNT powder.

Figure S2 shows TEM images of our BNNTs. In a) we see a low magnification image of two BNNTs. In b) we can see a high magnification image of a single BNNT confirming inner nanotube diameters are approximately 5 nm and that these samples are of high crystallinity as the nanotube wall fringes are clearly visible with a d-spacing of 0.33 nm.

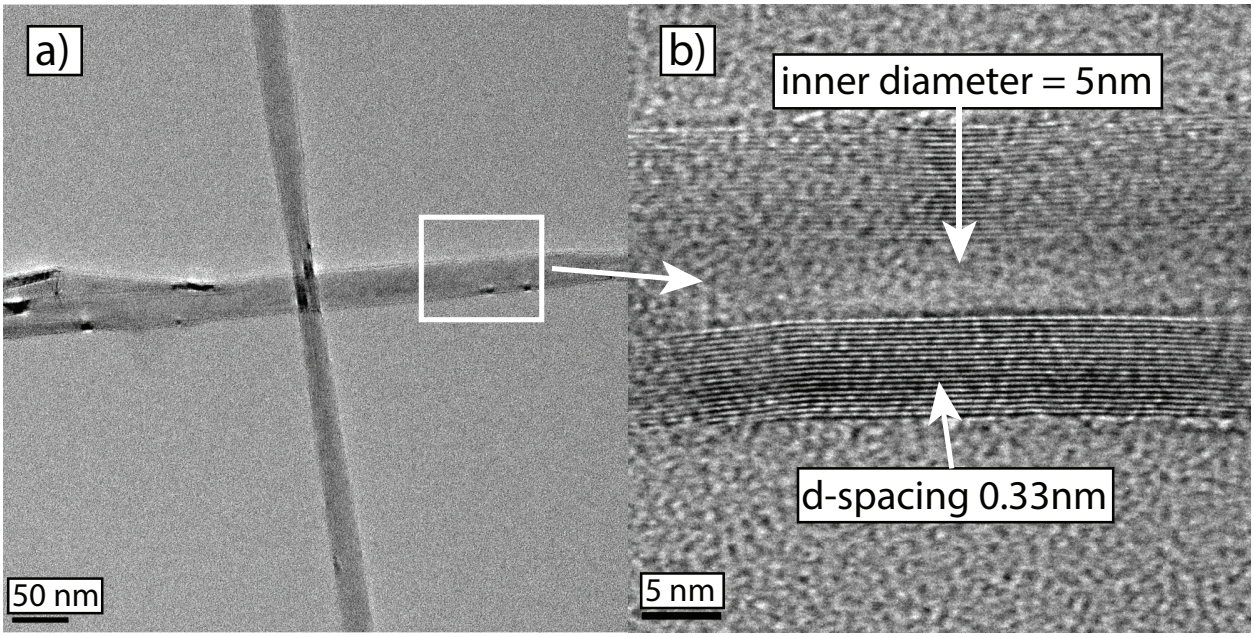

Figure S2: TEM images of BNNTs. a) shows lower magnification image with a scale bar showing 50 nm, while b) shows higher magnification with a scale bar of 5 nm.

Local Density of States

The local density of states (LDOS) can be calculated from dyadic Green function (or Green's tensor)[2,3]

$$\rho(z,\omega) = \left(2\omega/\left(\pi c^2\right)\right) Im\left(Tr\left(\overleftrightarrow{\mathbf{G}}\left(\mathbf{r},\mathbf{r}\right)\right)\right) \tag{1}$$

For a structure with infinite dielectric plane in the lower half space (z<0), the dyadic Green function in the upper half space (z>0) has been given by[4]

$$\overleftrightarrow{\mathbf{G}}\left(\mathbf{r},\mathbf{r}_0\right) = \overleftrightarrow{\mathbf{G}}_0\left(\mathbf{r},\mathbf{r}_0\right) + \overleftrightarrow{\mathbf{G}}_{\text{ref}}\left(\mathbf{r},\mathbf{r}_0\right) \tag{2}$$

$\overleftrightarrow{\mathbf{G}}_0$ and $\overleftrightarrow{\mathbf{G}}_{\text{ref}}$ are the the dyadic Green function in free space and the contribution due to reflection from the interface, respectively. The free space dyadic Green function can be obtained by

$$\overleftrightarrow{\mathbf{G}}_0\left(\mathbf{r},\mathbf{r}_0\right)=\frac{\mathbf{i}}{8\pi^2}\int_{-\infty}^{\infty}\overleftrightarrow{\mathbf{M}}\,\mathrm{e}^{\mathrm{i}\left[k_x(x-x_0)+k_y(y-y_0)+k_{z_1}|z-z_0|\right]}\mathrm{d}k_x\mathrm{d}k_y \tag{3}$$

Here k_0 is wave vector in vacuum, k_{z1} is the wave vector perpendicular to the interface in the upper half space.

$$k_x^2+k_y^2+k_{z1}^2=k_0^2, Im\left(k_{z1}\geq 0\right) \tag{4}$$

$\overleftrightarrow{\mathbf{G}}_0$ can be decomposed by splitting the matrix $\overleftrightarrow{\mathbf{M}}$ into an s-polarized part and a p-polarized part.

$$\overleftrightarrow{\mathbf{M}}\left(k_x,k_y\right)=\overleftrightarrow{\mathbf{M}}^{\,\mathrm{s}}\left(k_x,k_y\right)+\overleftrightarrow{\mathbf{M}}^{\,\mathrm{p}}\left(k_x,k_y\right) \tag{5}$$

The decomposition of the matrix can be expressed by

$$\overleftrightarrow{\mathbf{M}}^{\,\mathrm{s}}=\frac{1}{k_{z_1}\left(k_x^2+k_y^2\right)}\begin{bmatrix}k_y^2 & -k_xk_y & 0\\ -k_xk_y & k_x^2 & 0\\ 0 & 0 & 0\end{bmatrix} \tag{6}$$

$$\overleftrightarrow{\mathbf{M}}^{\,\mathrm{p}}=\frac{1}{k_1^2\left(k_x^2+k_y^2\right)}\begin{bmatrix}k_x^2k_{z_1} & k_xk_yk_{z_1} & \mp k_x\left(k_x^2+k_y^2\right)\\ k_xk_yk_{z_1} & k_y^2k_{z_1} & \mp k_y\left(k_x^2+k_y^2\right)\\ \mp k_x\left(k_x^2+k_y^2\right) & \mp k_y\left(k_x^2+k_y^2\right) & \left(k_x^2+k_y^2\right)^2/k_{z_1}\end{bmatrix} \tag{7}$$

Then, the reflected part of the dyadic Green function can be obtained by multiplying the s- and p- waves in $\overleftrightarrow{\mathbf{G}}_0$ with the corresponding Fresnel reflection coefficients r_s and r_p .

$$\overleftrightarrow{\mathbf{G}}_{\text{ref}}\left(\mathbf{r},\mathbf{r}_0\right)=\frac{\mathrm{i}}{8\pi^2}\int_{-\infty}^{\infty}\left[\overleftrightarrow{\mathbf{M}}_{\text{ref}}^{\,\mathrm{s}}+\overleftrightarrow{\mathbf{M}}_{\text{ref}}^{\,\mathrm{p}}\right]\mathrm{e}^{\mathrm{i}\left[k_x(x-x_0)+k_y(y-y_0)+k_{z_1}(z+z_0)\right]}\mathrm{d}k_x\mathrm{d}k_y \tag{8}$$

$$\overset{\leftrightarrow}{\mathbf{M}}_{\mathrm{ref}}^{\mathrm{s}}=\frac{r^{\mathrm{s}}\left(k_x,k_y\right)}{k_{z_1}\left(k_x^2+k_y^2\right)}\begin{bmatrix}k_y^2 & -k_xk_y & 0\\ -k_xk_y & k_x^2 & 0\\ 0 & 0 & 0\end{bmatrix} \tag{9}$$

$$\overset{\leftrightarrow}{\mathbf{M}}_{\mathrm{ref}}^{\mathrm{p}}=\frac{-r^{\mathrm{p}}\left(k_x,k_y\right)}{k_1^2\left(k_x^2+k_y^2\right)}\begin{bmatrix}k_x^2k_{z_1} & k_xk_yk_{z_1} & k_x\left(k_x^2+k_y^2\right)\\ k_xk_yk_{z_1} & k_y^2k_{z_1} & k_y\left(k_x^2+k_y^2\right)\\ -k_x\left(k_x^2+k_y^2\right) & -k_y\left(k_x^2+k_y^2\right) & -\left(k_x^2+k_y^2\right)^2/k_{z_1}\end{bmatrix} \tag{10}$$

For uniaxially anisotropic materials like hBN, the permittivity tensor is written as

$$\overset{\leftrightarrow}{\varepsilon}=\begin{bmatrix}\varepsilon_{\parallel} & 0 & 0\\ 0 & \varepsilon_{\parallel} & 0\\ 0 & 0 & \varepsilon_{\perp}\end{bmatrix} \tag{11}$$

The generalized Fresnel reflection coefficients for s- and p- waves turn out to be[2]

$$r^s=\frac{k_{z1}-k_{z2}}{k_{z1}+k_{z2}} \tag{12}$$

$$r^p=\frac{\varepsilon_{\parallel}k_{z1}-k_{ze}}{\varepsilon_{\parallel}k_{z1}-k_{ze}} \tag{13}$$

Here, k_{z2} and k_{ze} are perpendicular parts of wave vector for ordinary and extraordinary waves in the lower half space, respectively.

$$k_x^2+k_y^2+k_{z2}^2=\varepsilon_{\parallel}k_0^2, Im\left(k_{z2}\geq 0\right) \tag{14}$$

$$\frac{k_x^2+k_y^2}{\varepsilon_{\perp}}+\frac{k_{ze}^2}{\varepsilon_{\parallel}}=k_0^2, Im\left(k_{ze}\geq 0\right) \tag{15}$$

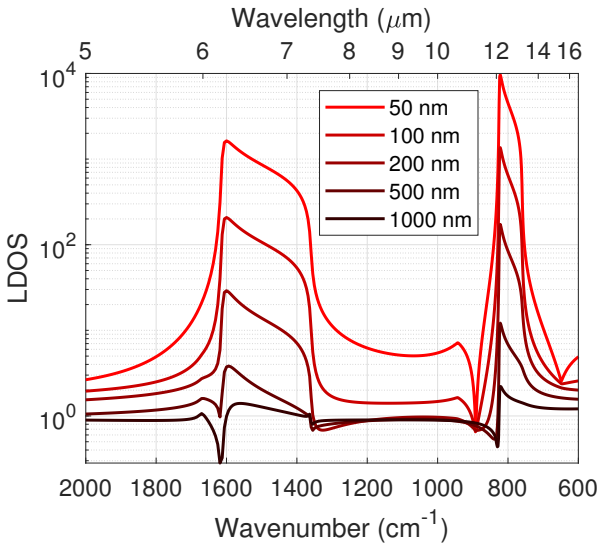

Figure S3: LDOS above a half space of hBN in vacuum.

Mie scattering of infinitely long cylindrical particle

To determine where the optical phonon modes exist in our BNNTs, we use Mie theory to calculate the absorption efficiency of an infinitely long isotropic cylinder for the two permittivities of hBN (shown in figure S4).[5,6] For figure S4 a), we consider light propagating perpendicular to the BNNT such that $\vec{k} \perp \vec{l_c}$ ($\vec{l_c}$ being the cylinder axis). In this orientation, we can have two polarizations of light, $\vec{E} \perp \vec{l_c}$ (TE) and $\vec{E} \parallel \vec{l_c}$ (TM).

Under TE excitation, we see two absorption peaks. The first TE peak, at 1573 cm^{-1}, is the tangential (T) mode and is the result of B-N stretching in the tangential direction (ε_t).[7,8] It is associated with the LO phonon in the ε_t direction and is generally not observed in hBN. The second TE peak, at 817 cm^{-1}, is due to the radial buckling (RB) mode of the nanotube where boron and nitrogen atoms oscillate in the radial direction (ε_r).[7] It is associated with the LO phonon in the ε_r direction.

Under TM excitation, we see a strong absorption peak at 1356 cm^{-1}. This is the longitudinal (L) mode of the nanotube which corresponds to the TO phonon of ε_a in hBN.[7,8] There is no absorption peak present in the lower Reststrahlen band for TM polarization because a radial permittivty which is a TE mode and cannot be excited with a TM wave.

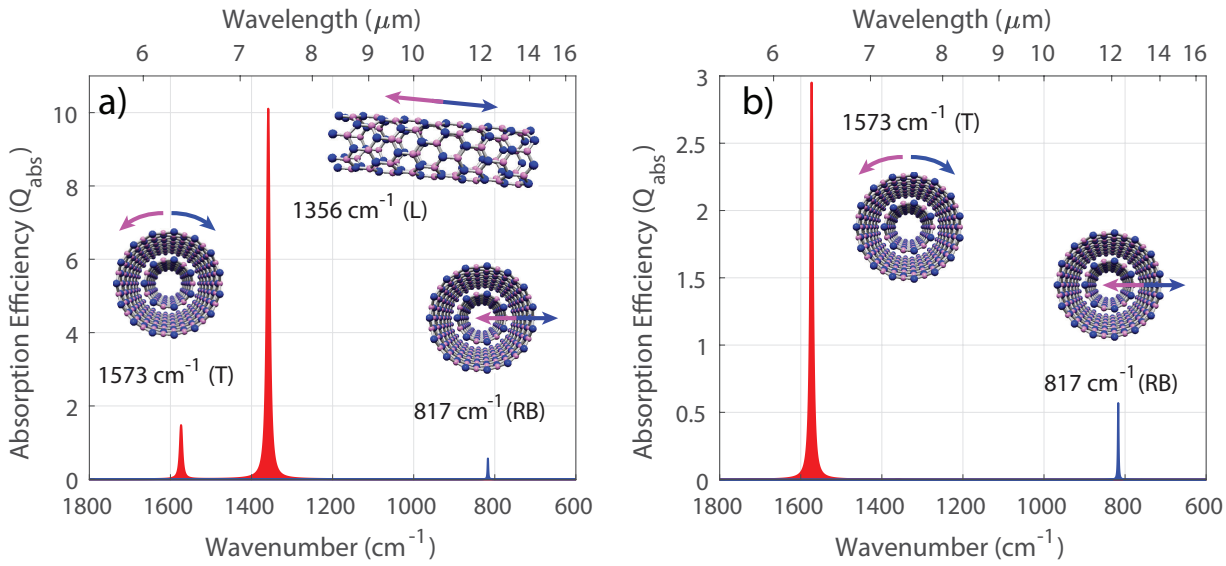

Figure S4: Mie absorption efficiency from infinite cylinder of hBN permittivities for a) perpendicular incidence and b) axial incidence.

For cylindrical shaped particles with high aspect ratio, we can approximate the scattering and absorption widths as that for an infinitely long cylinder. If we consider normal incidence (light propogating perpendicular to the cylinder axis z), we can have two polarizaton states

(i) $E \parallel z$

$$C_{sca} = \frac{2}{k_0 r} \sum_{n=-\infty}^{n=\infty} |b_n|^2 \,, \tag{16}$$

$$C_{abs} = \frac{2}{k_0 r} \sum_{n=-\infty}^{n=\infty} (-Re\, b_n - |b_n|^2) \,, \tag{17}$$

$$C_{ext} = -\frac{2}{k_0 r} \sum_{n=-\infty}^{n=\infty} (Re\, b_n) \,, \tag{18}$$

with

$$b_n = \frac{k_i J_n'(k_i r) J_n(k_0 r) - k_0 J_n(k_i r) J_n'(k_0 r)}{k_0 J_n(k_i r) H_n'(k_0 r) - k_i J_n(k_i r) H_n(k_0 r)} \,, \tag{19}$$

where $k_0 = \varepsilon_M^{1/2}\omega/c$, $k_i = \varepsilon^{1/2}\omega/c$ are spherical harmonics and J_n and H_n are cylindrical Bessel and Hankel functions respectively.

(ii) $E \perp z$

$$C_{sca} = \frac{2}{k_0 r} \sum_{n=-\infty}^{n=\infty} |a_n|^2 \,, \tag{20}$$

$$C_{abs} = \frac{2}{k_0 r} \sum_{n=-\infty}^{n=\infty} (-Re\, a_n - |a_n|^2) \,, \tag{21}$$

$$C_{ext} = -\frac{2}{k_0 r} \sum_{n=-\infty}^{n=\infty} (Re\, a_n) \,, \tag{22}$$

with

$$a_n = \frac{k_i J_n(k_i r) J_n'(k_0 r) - k_0 J_n'(k_i r) J_n(k_0 r)}{k_0 J_n'(k_i r) H_n(k_0 r) - k_i J_n(k_i r) H_n'(k_0 r)} \,. \tag{23}$$

Following these equations we can calculate the scattering, absorption and extinction efficiencies as

$$Q_b = \frac{C_b}{2r} \,, \tag{24}$$

where $b = abs, sca, ext$. The methodology for calculating the absorption, scattering and extinction efficiency of cylindrical particles is taken from.[6,9]

References

(1) Starko-Bowes, R.; Dai, J.; Newman, W.; Molesky, S.; Qi, L.; Satija, A.; Tsui, Y.; Gupta, M.; Fedosejevs, R.; Pramanik, S.; Xuan, Y.; Jacob, Z. *Journal of Quantitative Spectroscopy and Radiative Transfer* **2018**, *216*, 99 – 104.

(2) Guo, Y.; Cortes, C. L.; Molesky, S.; Jacob, Z. *Applied Physics Letters* **2012**, *101*, 131106.

(3) Cortes, C. L.; Newman, W.; Molesky, S.; Jacob, Z. *Journal of Optics* **2012**, *14*, 063001.

(4) Novotny, L.; Hecht, B. *Principles of nano-optics*; Cambridge university press, 2012.

(5) Kerker, M. *The scattering of light and other electromagnetic radiation*; Academic Press, 1969.

(6) Bohren, C. F.; Huffman, D. *Absorption and scattering of light by small particles*; Wiley science paperback series; Wiley, 1983.

(7) Wirtz, L.; Rubio, A.; de la Concha, R. A.; Loiseau, A. *Phys. Rev. B* **2003**, *68*, 045425.

(8) Lee, C. H.; Wang, J.; Kayatsha, V. K.; Huang, J. Y.; Yap, Y. K. *Nanotechnology* **2008**, *19*, 455605.

(9) Ruppin, R.; Englman, R. *Reports on Progress in Physics* **1970**, *33*, 149.